

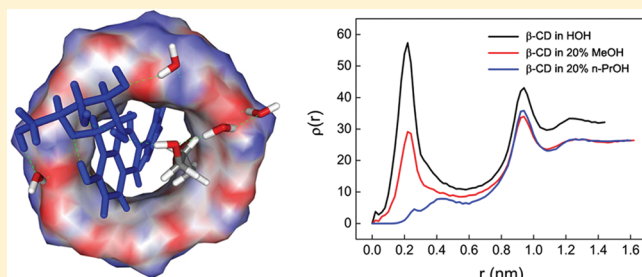
Insight into the Structural Deformations of Beta-Cyclodextrin Caused by Alcohol Cosolvents and Guest Molecules

Haiyang Zhang^{†,‡} Chunling Ge,[†] David van der Spoel,[‡] Wei Feng,[†] and Tianwei Tan^{*,†}

[†]Beijing Key Lab of Bioprocess, College of Life Science and Technology, Beijing University of Chemical Technology, Box 53, 100029 Beijing, China

[‡]Department of Cell and Molecular Biology, Uppsala University, Husargatan 3, Box 596, SE-751 24 Uppsala, Sweden

ABSTRACT: Beta-cyclodextrin (β -CD) is an ideal candidate for a host molecule, and it is used as such in drug delivery and separation technology. The structural behavior of free β -CD and host–guest complexes of β -CD with two isoflavonoid isomers (puerarin and daidzin) in aqueous alcohol solutions, covering methanol, ethanol, 2-propanol, and 1-propanol, was investigated through molecular dynamics (MD) simulations. The MD results highlighted aspects of the structural flexibility and rigidity of β -CD in different alcohol solutions. The alcohol residence time within the β -CD cavity, solvent distribution around β -CD, and guest-induced structural changes were analyzed. Interaction with puerarin endowed β -CD with a more rigid structure than with daidzin and a weaker ternary complex β -CD/puerarin/alcohol was formed with a local participation of water molecules. The retention behavior of puerarin and daidzin on a β -CD-coupled medium was determined via chromatographic experiments and simulation results provided a structural explanation for such interactions.



1. INTRODUCTION

Cyclodextrins (CDs) have attracted considerable attention over the years due to the many interesting applications related to host–guest complex formation. As a family of cyclic oligosaccharides typical cyclodextrins are composed of six, seven, or eight glucose monomers in a ring, denoted as alpha-, beta-, and gamma-cyclodextrin (α , β , and γ -CD for short, respectively) in order of increased size, and they can be topologically represented as truncated cones.^{1–3} The structure of β -CD is schematically shown in Figure 1a. The interior of the cone is lined with methine protons and lone pairs of glycosidic oxygen atoms, creating a somewhat hydrophobic cavity.^{4,5} In contrast, hydroxyl groups situated at the primary and secondary rim endow cyclodextrins with hydrophilic character. The cavity permits inclusion of nonpolar guest molecules in whole or in part while polar moieties of the guest can simultaneously interact with the surface hydroxyls, if sterically possible. Formation of inclusion complexes provides an alternative to modification of physical and chemical properties of guest molecules, mostly in terms of water solubility. This property of CDs leads to practical applications in many fields, like pharmaceuticals,⁶ the food industry,⁷ cosmetics,⁸ and agriculture⁹ as well as in separation science¹⁰ and environmental protection.¹¹ In addition, CDs can be used as enzyme models,^{12,13} allowing one to mimic the interaction of an enzyme with a substrate.

Guest inclusion and release are of fundamental importance to the application of CDs. The major driving forces responsible for the formation and stabilization of complexes are van der Waals, hydrophobic, and hydrogen bond interactions between

natural cyclodextrins and guest molecules.¹⁴ The release of strain energy in the cyclodextrin ring and displacement of high-energy water from the cavity have been suggested to contribute to binding as well.^{15,16} On the basis of X-ray and neutron diffraction data, Saenger and co-workers¹³ proposed an “induced-fit”-like mechanism for complex formation of the enzyme model α -CD with varied substrates and concluded that formation of α -CD/substrate complex was mainly owing to a change in conformation and hydrogen bonding of the α -CD molecule itself. Dodziuk⁵ reported a review of experimental and theoretical studies on the CD flexibility and indicated that weak host–guest interactions can limit the macrocycle flexibility somewhat but can not endow CDs with rigidity.

Organic solvents like alcohols can affect CD-guest interactions and cause changes in the complex stability, something which can be exploited for a specific purpose. Short-chain alcohols often act as cosolvents in the eluent to obtain efficient separations in the CD-aided chromatography.^{17–19} Liu et al. reported an interesting experiment where a small amount of methanol and ethanol decreased the binding constant of a β -CD dimer toward the dye acridine red, whereas 2-propanol had the opposite effect.²⁰ They speculated that 2-propanol would extrude a larger amount of water from the β -CD cavity and give a favorable enhancement of the hydrophobic interaction between β -CD and its guest. Warner et al. concluded, based on fluorescence lifetime measurements,

Received: January 19, 2012

Revised: February 28, 2012

Published: February 29, 2012

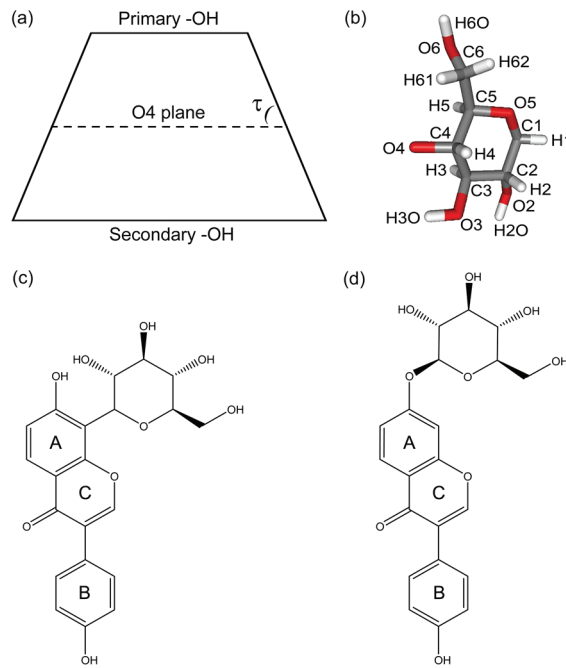


Figure 1. Schematic representation of β -CD (a), stick models of one glucose monomer in β -CD (b) and two isoflavone glycosides puerarin (c) and daidzin (d). Tilt angle τ of one glucose unit is defined as the angle between two least-squares best-fit planes, O4 plane and the glucose ring plane through C1–C2–C3–C4–C5–O5. Three rings in the isoflavone backbone are marked A, B, and C, respectively.

that the presence of methanol, ethanol, 2-propanol, and 1-propanol induced a longer lifetime of the γ -CD/pyrene inclusion complex than a pure water solvent due to local participation of alcohol in the γ -CD/pyrene complex.²¹ Hamai confirmed the formation of a ternary 1:1:1 inclusion compound between β -CD/pyrene and primary or cyclic alcohols in aqueous solutions, by fluorescence absorption spectroscopy.²² Bohne et al. found that the addition of alcohol led to the formation of a weaker ternary complex compared to the β -CD/xanthone binary complex but to a slight increase of the complexation strength for γ -CD.²³ These experimental results demonstrate that alcohols can be used to fine-tune stability and dynamics of CD-guest complexes, which may have implications for the applications of CDs in drug delivery and separation technology. The mechanism behind such phenomena needs to be fully understood in order to selectively control the properties of CD complexes.

Molecular dynamics (MD) simulation is a useful supplement to experiments that can provide a deeper understanding of the behavior of free CDs and CD-based complexes at the molecular level.^{4,16,24,25} Many research groups have performed MD simulations in aqueous solution to investigate the hydration and flexibility of CDs and to explore the anomalous solubility of β -CD, relative to α -CD and γ -CD.^{26–32} However, there have been few reports concerning MD study of CDs in alcohol solutions. In a recent paper, Lawtraku and co-workers studied the behavior of β -CD in methanol, ethanol, and their aqueous solutions using MD simulations and characterized the number and location of encapsulated solvents inside the β -CD cavity.³³

Here, we report a systematic computational study on structural changes of free β -CD molecule and β -CD/guest complexes in aqueous alcohol solutions, including methanol, ethanol, 2-propanol, and 1-propanol. Two isoflavonoid isomers (puerarin and daidzin) are selected as guest molecules to

explore guest-induced structural changes. The IUPAC name for puerarin is 7-hydroxy-3-(4-hydroxyphenyl)-8-[$(3R,4R,5S,6R)$ -3,4,5-trihydroxy-6-(hydroxymethyl)oxan-2-yl]chromen-4-one and for daidzin 3-(4-hydroxyphenyl)-7-[$(2S,3R,4S,5S,6R)$ -3,4,5-trihydroxy-6-(hydroxymethyl)oxan-2-yl]oxychromen-4-one. These two substances whose structures are shown in Figure 1c,d are widely used in traditional Chinese medicine³⁴ and are difficult to separate from each other due to structural similarity. Following our previous study,³⁵ we determine via high-performance liquid chromatography (HPLC) the retention behavior of puerarin and daidzin on a β -CD-coupled stationary phase using a mixed eluent of water and alcohols. In this work, we focus on the structural deformations of β -CD caused by alcohol and the two guests and on the solvent distribution around β -CD and aim to provide a structural explanation for such interactions.

2. EXPERIMENTAL SECTION

2.1. Computational Methods.

2.1.1. Simulation Protocol. The initial coordinate of β -CD was extracted from the crystal structure (PDB code: 1DMB).³⁶ Atomic point charges for one glucose unit in β -CD for the water phase were taken from work by Cai and co-workers,³⁰ who used a continuum description of the environment and considered the molecular symmetry of CDs to compute charges at the B3YLP/6-311+ + (G,P) level of theory. The restrained electrostatic potential (RESP) charges of methanol (MeOH), ethanol (EtOH), 2-propanol (isopropanol, i-PrOH), 1-propanol (*n*-PrOH), puerarin (P) and daidzin (D) were derived by fitting partial charges to electrostatic potentials calculated by the Gaussian 03 program³⁷ at the HF/6-31G* level of theory with the aid of the AMBER 10 software.³⁸ The GLYCAM06³⁹ force field was used to model β -CD and the general AMBER force field (GAFF)⁴⁰ was used for alcohols, puerarin, and daidzin. These AMBER topology and structure files were further converted to the GROMACS format via amb2gmx.pl script.⁴¹

The AMBER force fields have been validated for use in the GROMACS package.^{42,43} The default factors of 1/2 and 1/1.2 were applied to scale 1–4 Lennard-Jones and electrostatic interactions, as described by the AMBER all-atom potentials,⁴⁴ whereas the GLYCAM06 force field parameters for carbohydrates were derived without scaling these interactions. For consistency with the GAFF parametrization we used the scaled 1–4 nonbonded interactions, as indicated by the AMBER manual when the AMBER and GLYCAM force fields coexisted. Note that for isolated carbohydrates both scaling factors should be set to unity in order to properly treat internal hydrogen bonds, particularly those associated with the hydroxymethyl group, and to correctly reproduce the rotamer populations for the C5–C6 bond.^{39,45} We simulated the isolated β -CD solvated in water, with and without scaling 1–4 nonbonded interactions. In the X-ray crystallized structure,⁴⁶ four of seven C6–O6 bonds in β -CD are rotated outward [called (–) gauche orientation] from the cavity, two C6–O6 bonds are inward [(+) gauche], and the other one is 2-fold disordered over these two orientations. During the simulation, the occupancy for (–) gauche is 0.1–0.4 with scaling and 0.3–0.6 without scaling; the latter one is closer to the X-ray structure.

All simulations were performed with the rigid water model TIP3P,⁴⁷ using the GROMACS^{48,49} package, version 4.5.3. Periodic boundary conditions in all directions were taken into account to minimize edge effects in a finite system. Prior to each simulation, an energy minimization using a steepest

descent algorithm was performed to avoid bad contacts. In order to maintain the temperature at 300 K and the pressure at 1 bar, the velocity rescaling thermostat⁵⁰ and Parrinello-Rahman barostat^{51,52} were used with coupling constants of 0.1 and 5 ps, respectively, for the temperature and pressure coupling. Long-range electrostatic interactions were treated using the particle mesh Ewald approach^{53,54} with a cutoff distance of 1.0 nm. Lennard-Jones interactions were cutoff at 1.4 nm. Neighbor lists were updated every 10 steps, and constraints were applied for all bonds using the LINCS algorithm⁵⁵ for β -CD, puerarin, daidzin, and alcohols, and SETTLE⁵⁶ for water. Atomic trajectories were propagated by integrating classical Newton's equations of motion using the Leap-Frog algorithm with a time step of 0.002 ps, and coordinates were saved to disk every 1 ps. The (nonbonded) interaction energy between host (or guest) and solvents is defined as the sum of Lennard-Jones and Coulomb energy terms that are computed on the basis of a neighbor list with removal of exclusions. Analyses were carried out using the programs within the GROMACS package.

2.1.2. Equilibration of Alcohol Solvents. For each alcohol species a cubic box containing 600 molecules was created and equilibrated by 5-ns MD simulations. The final coordinate was saved as a solvent box for further use. The last 3-ns trajectories were used to calculate simulated densities, which are in good agreement with experimental values, as shown in Table 1,

Table 1. Comparison of Experimental Density (g/mL) with the Simulated Value for Parameterized Alcohol Models (Relative Standard Deviations in Parentheses)

alcohol	exp. density	sim. density	log P^a
MeOH	0.79	0.80 (1.13%)	-0.77
EtOH	0.79	0.79 (0.94%)	-0.31
i-PrOH	0.79	0.80 (0.72%)	0.05
n-PrOH	0.80	0.81 (0.74%)	0.25

^a P , *n*-octanol/water partition coefficients calculated by ALOGPs 2.1^{57,58}

where the *n*-octanol/water partition coefficients were calculated by ALOGPs 2.1.^{57,58}

2.1.3. Production Simulation. Before each production a 10 ps simulation was performed with position restraints on the β -CD molecule to allow solvent equilibration. One free β -CD molecule was simulated in 0%, 20%, 50%, and 100% (v/v) alcohol solvents. The first three solvents contained 800 water molecules and a different number of alcohol molecules. To analyze residence of alcohols within the β -CD cavity, we performed simulations of one β -CD in a mixed solvent of 10 alcohol molecules and 790 water molecules. Initial structures of inclusion complexes of puerarin (P) and daidzin (D) with β -CD in water were taken from our previous study.⁵⁹ The β -CD/P and β -CD/D complexes were simulated in water and 20% alcohols. To test reproducibility each system was run twice with different initial velocities generated from a Maxwell distribution at 300 K with a random seed. Each simulation was extended to 10 ns and the last 4 ns was used for data collection unless stated otherwise.

2.2. HPLC Determination. A column packed with β -CD-coupled polymer particles was used in the chromatographic experiments to determine the retention time of puerarin and daidzin. Alcohol–water solutions with concentration ranging from 15% to 100% (v/v) were used as the mobile phases.

Materials and operation conditions at room temperature were the same as in our previous report.³⁵

3. RESULTS AND DISCUSSION

3.1. Structural Change of Free β -CD. The root-mean-square deviations (RMSDs) of β -CD from the crystal structure are computed with mass weighting for superposition and shown in Figure 2 for water (HOH) and pure alcohol

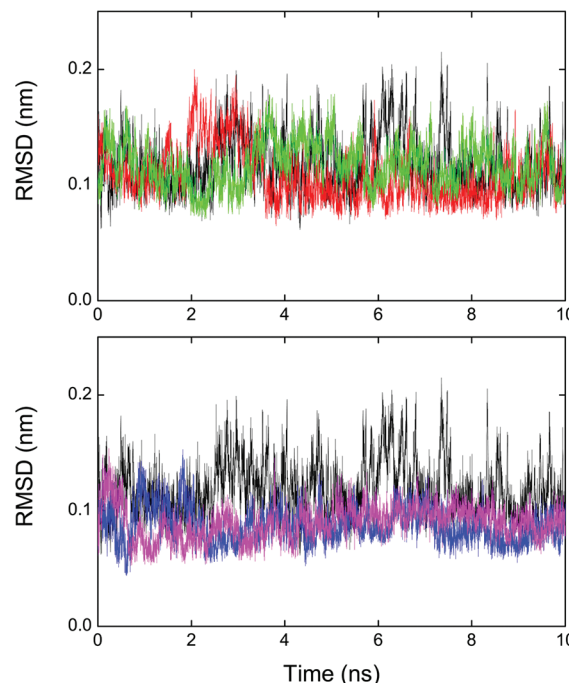


Figure 2. Root-mean-square deviation (RMSD) of β -CD from the crystal structure during 10-ns simulations in pure liquids of water (black), MeOH (red), EtOH (green), i-PrOH (blue), and n-PrOH (magenta).

solutions. After equilibration the RMSD of all atoms of β -CD amounts to 0.12 ± 0.03 nm in water and is similar to that in pure alcohols, namely 0.10 ± 0.02 nm for methanol (MeOH), 0.11 ± 0.01 nm for ethanol (EtOH), 0.08 ± 0.01 nm for 2-propanol (i-PrOH), and 0.09 ± 0.01 nm for 1-propanol (n-PrOH). There are no significant differences in RMSDs of free β -CD for 20% and 50% alcohols. To further explore structural changes of β -CD, the root-mean-square fluctuations (RMSFs) of atomic positions from the crystal structure are calculated with mass weighting and shown in Figure 3. Atom names of the repeating unit of one glucose monomer in β -CD are marked in Figure 1b. For all solutions studied the RMSF value of β -CD is smaller for higher alcohol concentration than dilute solution. Compared to water, β -CD shows smaller structural changes in 100%, 50% alcohols, and 20% i-PrOH and 20% n-PrOH. However, in 20% MeOH and 20% EtOH, β -CD displays similar or even larger fluctuations than in water.

As expected, primary hydroxyls in all solutions bear larger fluctuations than secondary ones and the heavy (non-hydrogen) atoms have smaller fluctuations. The H3 and H5 atoms that point inward to the cavity are not so affected by solvent as other nonpolar hydrogen atoms (H1, H2, and H4) exposed to the environment and hence have smaller fluctuations. In contrast to the situations in water and dilute

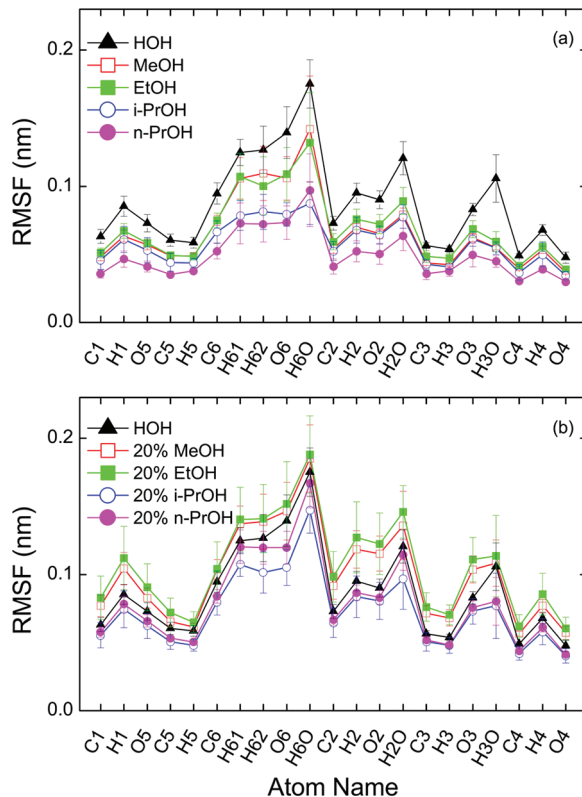


Figure 3. Root-mean-square fluctuation (RMSF) of atomic positions of β -CD from the crystal structure in pure liquids (a) and in 20% alcohol (b). Error bars refer to the standard deviation based on seven glucose units.

alcohol solutions, fluctuations of the H3O atom in pure alcohols are smaller than O3, due to the presence of strong intramolecular hydrogen bonds between adjacent secondary hydroxyl groups belonging to different glucose residues. These hydrogen bonds were classified into types A, B, and C.³² Type A looks like O2—H2O···O3—H3O, type B is H2O—O2···H3O—O3, and type C is a rapid exchange hydrogen bond (known as “flip-flop”⁶⁰) flipping from type A to type B or vice versa. Hydrogen bonds are determined from the trajectories using a geometrical criterion based on cutoffs with a donor–acceptor distance of at most 0.35 nm and an acceptor–donor–hydrogen angle of at most 30°. OH groups are regarded as donors and O as an acceptor. In the aqueous simulation all the three types of hydrogen bonds exist and type B occurs with a higher probability than type A, in agreement with a report by Naidoo and co-workers.³² In pure alcohols hydrogen bonds are almost always type B, which limits movement of the H3O atom and endows it with a smaller fluctuation.

Structural changes of β -CD in alcohol solutions can be explained by intramolecular hydrogen bonds at the secondary rim and by interactions between β -CD and solvent molecules, as shown in Figure 4. Compared to the dilute alcohol solutions, the secondary hydroxyls of β -CD tend to form more intramolecular hydrogen bonds in higher concentration. In pure alcohols all seven intramolecular hydrogen bonds are observed with smaller deviations (Figure 4a). These hydrogen bonds were reported to contribute partly to its relative rigid macrocycle structure and anomalous solubility.^{27,30} The interaction energy between β -CD and solvents is more negative for dilute solutions than for higher concentration; in

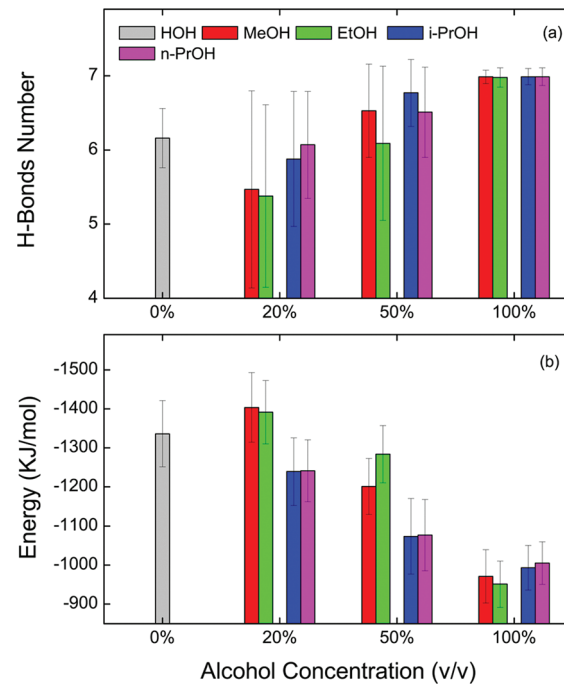


Figure 4. Number of intramolecular hydrogen bonds between adjacent secondary hydroxyls of β -CD (a) and the interaction energy between β -CD and solvent molecules (b).

20% MeOH and 20% EtOH the interaction energies are slightly more negative than in water (Figure 4b). There is a correlation between the stronger interaction with solvents and the larger fluctuation in the β -CD structure.

3.2. Alcohol Residence within Cavity. In MD simulations alcohol molecules can enter the β -CD cavity, stay there for some time, and then escape again, allowing residence of another molecule. The molecule within the cavity can be defined by a radius from the centroid of β -CD. Here we calculate the distance between the carbon atom in the methyl group of alcohol and the centroid of β -CD to track the residence of alcohol. The alcohol molecule whose methyl group stays within a sphere with a radius of 0.4 nm is considered to be inside the cavity and marked by its index. The i-PrOH molecule is considered to be within the cavity if any one of the two methyl carbons is within the radius.

Figure 5 shows alcohol indexes within the β -CD cavity versus the simulation time. There are 10 alcohol molecules (0–9) in the system. Alcohols studied are not large enough to occupy the whole cavity and hence the cavity can simultaneously accommodate more than one molecule. As expected, nonpolar molecules have a longer residence time within the hydrophobic cavity than polar ones during the simulation. MeOH shuttles freely inside the cavity but does not stay within it for a long time because of its lower Log P value (Table 1), i.e., higher polarity. The i-PrOH molecule with the index of 3 behaves similar to n-PrOH with the index of 2. However, n-PrOH is more easily bound to the cavity when another n-PrOH is already incorporated into the cavity (Figure 5d), which can be ascribed to the linearity of n-PrOH. The branched structure of i-PrOH effectively occupies more space in the cavity and other molecules that try to enter the cavity accommodating one i-PrOH molecule may be pushed out to some extent.

3.3. Solvent Distribution. The solvent distribution can be characterized by the radial distribution function, which provides

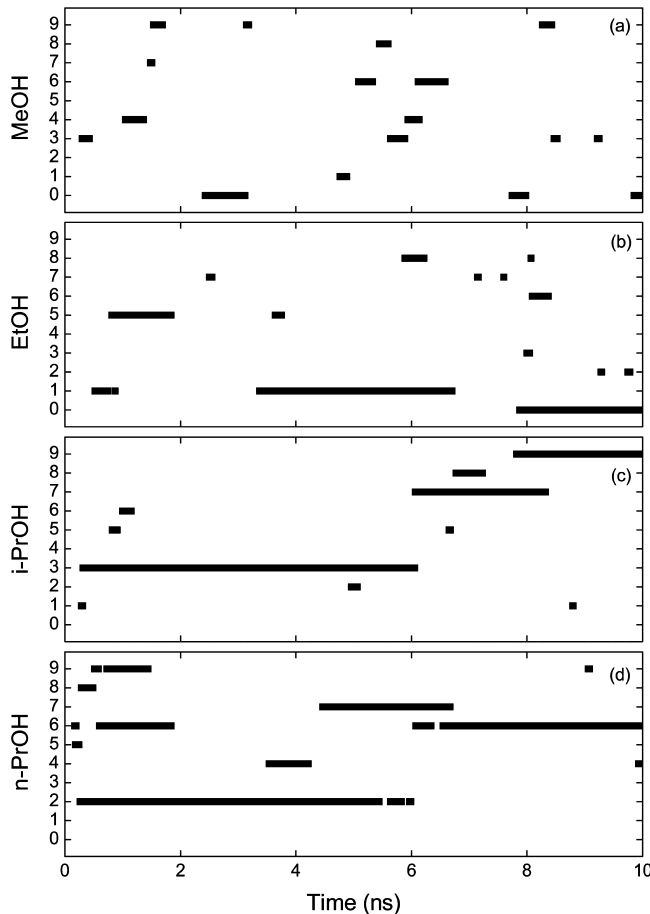


Figure 5. Index of alcohol within the β -CD cavity versus the simulation time. There are 10 alcohol molecules in the system and the alcohol molecule within the cavity is marked by its index (0–9).

valuable information on how solvent molecules are distributed inside and around β -CD. To be able to compare different systems here we use the non-normalized form $\rho(r)$, which gives

the probability density of finding a given group at a distance r from the centroid of β -CD. $\rho(r)$ is defined as $\rho(r) = n(r)/(4\pi r^2 \Delta r)$, where $n(r)$ is the average number of the given group in a spherical shell with thickness Δr at a distance r .²⁶

The average density $\rho(r)$ of oxygen in HOH, carbon in $-\text{CH}_3$ and oxygen in $-\text{OH}$ around β -CD in water and 20% alcohol are calculated and shown in Figure 6. As seen in Figure 6a, two peaks are observed in water (HOH), corresponding to water molecules within the cavity at about 0.2 nm and bound to the outer surface at about 0.9 nm, respectively. These water molecules form the first hydration shell of β -CD.³⁰ The number of encapsulated water molecules averaged over ten independent runs (5 ns each) in water is 6.9 ± 0.2 , in good agreement with neutron diffraction⁶⁰ and X-ray⁴⁶ experiments in which they observed about 6.5 water molecules. When interacting with β -CD, the methyl group of alcohol tends to enter and stay within the hydrophobic cavity, whereas the hydroxyl group of alcohol prefers to interact with the surface hydroxyls of β -CD. Addition of cosolvent alcohols decreases the average density of water in the first solvation shell. In 20% i-PrOH and 20% n-PrOH there is only a very small peak within the cavity (Figure 6a), indicating that water molecules are almost extruded from the cavity by alcohol. Interestingly, an obvious peak occurs at about 0.4 nm, i.e., the boundary of the cavity, which proves rationality of the cutoff distance of 0.4 nm mentioned above. For the sake of clarity, we define three categories to describe the three peaks of solvent distribution: within the cavity (less than 0.4 nm), near the cavity boundary (about 0.4 nm) and near the outer surface (about 0.9 nm).

Figure 6, panels b and c, shows that the methyl group of alcohol has a higher density within the cavity and is much further away from β -CD near the outer surface than the hydroxyl of alcohol, revealing the hydrophobic environment of the cavity and hydrophilic surface at the two rims of β -CD. The methyl groups of i-PrOH and n-PrOH have a higher density within the cavity than those of MeOH and EtOH (Figure 6b). Due to the different molecular structure the hydroxyl of i-PrOH is much closer to the centroid of β -CD than n-PrOH

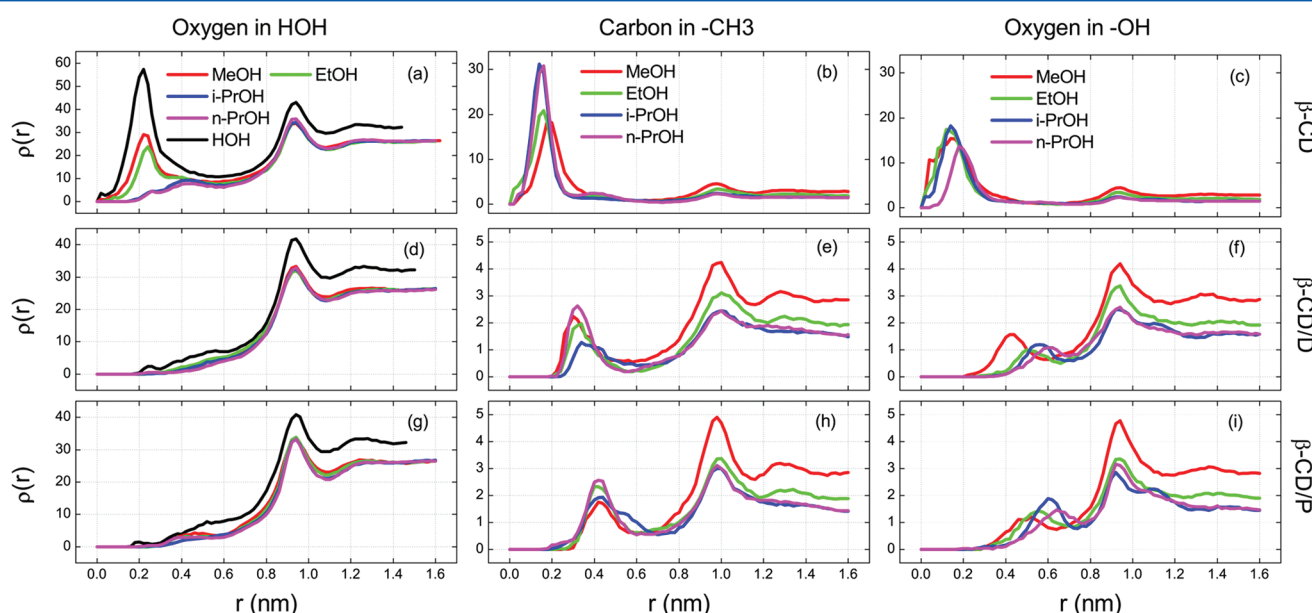


Figure 6. Water and alcohol distribution around β -CD for the free β -CD (top), β -CD/D (middle), and β -CD/P (bottom) systems in water and 20% alcohol. $\rho(r)$ is the average density of solvent molecules at a distance r from the centroid of β -CD. Distributions of the oxygen atom in HOH (left), carbon in $-\text{CH}_3$ (middle) and oxygen in $-\text{OH}$ (right) are computed for all systems.

(Figure 6c). In 50% alcohol solutions the cavity is almost completely occupied by alcohol and water molecules are predominantly located at the outer surface with a lower density than in 20% alcohol solutions.

When a guest molecule (D or P) is bound to the β -CD cavity, solvent distributions differ from free β -CD, as shown in Figure 6d–i. The cavity is already occupied by the guest and thus solvents including alcohol and water molecules can not get into the cavity. All alcohols lead to a decrease in the average density of water around β -CD but not to significant differences in water distribution (Figure 6, panels d and g). For the alcohol distribution, we first discuss the case near the cavity. In the β -CD/D system the methyl group of alcohol is still within the cavity but not as close to the centroid of β -CD (Figure 6e) as it is in the free β -CD system. In the β -CD/P system, however, the methyl of alcohol does not fit within the cavity and is located near the cavity boundary (Figure 6h). For the β -CD/D and β -CD/P systems the hydroxyl of alcohol is located slightly

further away from the cavity boundary and MeOH is much closer to the boundary (Figure 6, panels f and i) because of its small size and high polarity. Near the outer surface the average density of the methyl and hydroxyl of alcohol in the β -CD/P system is slightly larger than that in the β -CD/D system, which may be due to stronger interactions between P and solvents. For the complex the interaction energy between P and solvents is -328 ± 34 kJ/mol and between D and solvents -286 ± 30 kJ/mol, respectively. There are no significant differences in the guest-solvent interaction energies for different alcohol solutions. MeOH has the largest density near the outer surface because all 20% (v/v) alcohols studied share the same number of water molecules and 20% MeOH has the largest number of alcohol molecules.

3.4. Guest-Induced Structural Change. To explore guest-induced effects, we analyzed distributions of the distances (L) and the tilt angles (τ) of glucose monomers and took the systems in 20% MeOH and 20% n-PrOH as the example (Figure 7a–d). The case in 20% EtOH is similar to

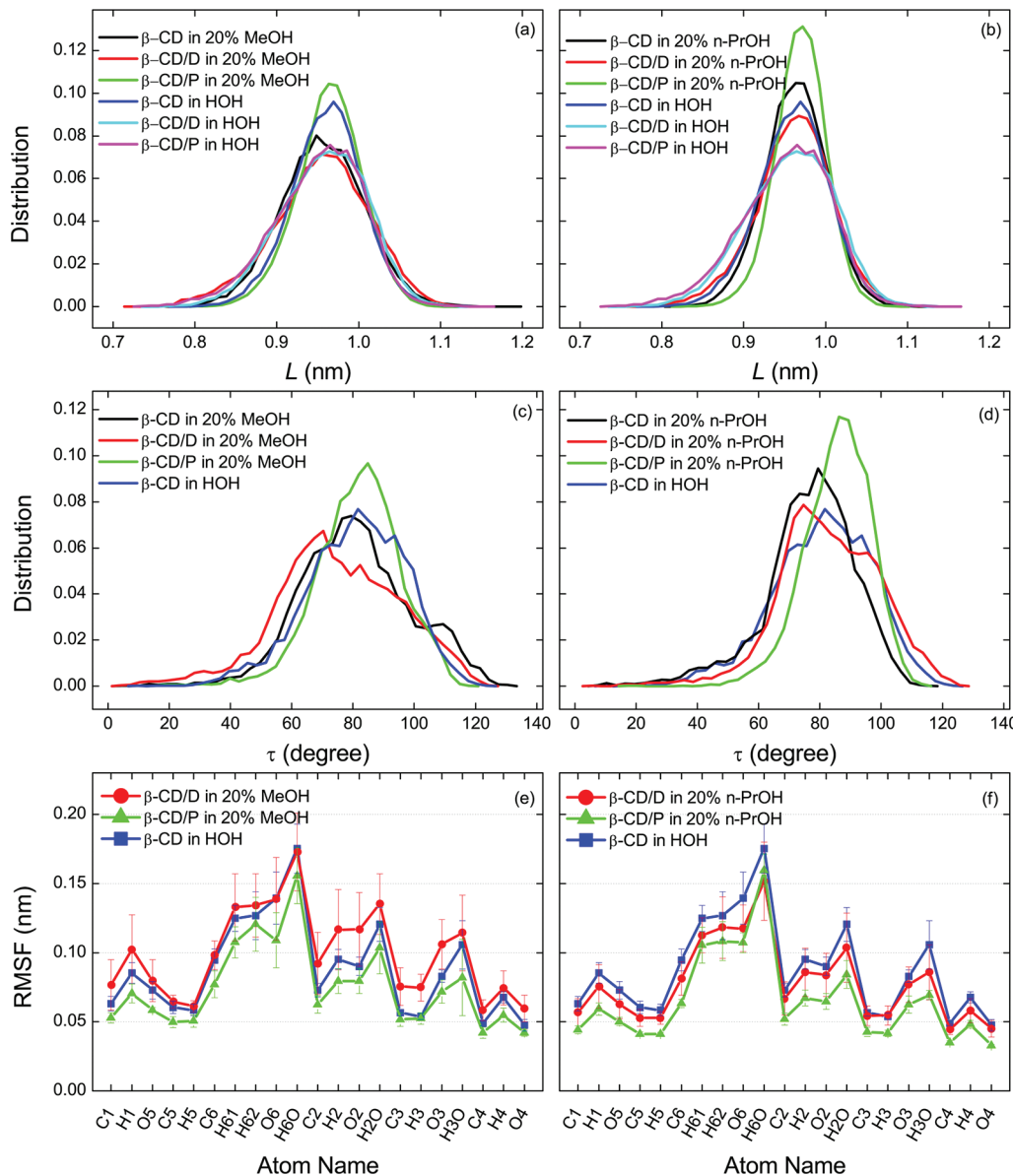


Figure 7. Distribution of the distance L (top) and the tilt angle τ (middle) and the RMSF plot of β -CD (bottom) for the β -CD, β -CD/D, and β -CD/P systems in 20% MeOH (left) and 20% n-PrOH (right). Data in water are shown here for comparison. Error bars refer to the standard deviation based on seven glucose units.

20% MeOH, and 20% i-PrOH is similar to 20% n-PrOH. L are distances of seven sets between each glycosidic oxygen atom and the midpoint of two opposing glycosidic oxygens and can be used to detect the distortion of the cavity. As noted earlier,⁵⁹ the cavity can be compressed in one direction and stretched in the other due to binding daidzin or puerarin where larger distortion corresponded to stronger host–guest interaction. Similarly, sharper distribution of L means more circular shape of the cavity (i.e., a rigid structure) and weaker binding of guest to host.

For free β -CD in 20% MeOH the distribution of L has a lower and wider profile, while in 20% n-PrOH it is slightly higher and narrower than in HOH, indicating a flexible structure of β -CD in 20% MeOH and a more rigid one in 20% n-PrOH as discussed in section 3.1. For the complex in 20% MeOH, interaction of β -CD with daidzin results in a flexible structure of β -CD, similar to β -CD/D and β -CD/P in HOH; however, interaction with puerarin leads to a rigid β -CD (Figure 7a). In 20% n-PrOH, interactions with daidzin and puerarin both give β -CD a more rigid structure than in HOH (Figure 7b). For the β -CD/P complex, L displays a sharper landscape in 20% n-PrOH than in 20% MeOH. No notable differences in the tilt angle are observed, while puerarin makes the tilt angle shift slightly to a bigger value (Figure 7, panels c and d). Structural changes of β -CD can be presented by the RMSF plot (Figure 7, panels e and f) where puerarin leads to smaller fluctuations than daidzin. These structural deformations upon variation of the alcohol and guest were studied by principal component analysis (PCA) as well. The vector components per atom of eigenvectors pinpoint the individual atomic fluctuations, similar to the RMSF plot. The three highest-eigenvalue principal components together describe more than 50% of the total atomic motion in all cases. The largest deformation modes involve the relative orientation of the glucose monomers and the shape of the cavity, related to the tilt angle (τ) and the distance (L) as mentioned above, respectively. The information about structural changes detected by PCA confirms what was reported in Figures 3 and 7.

The interaction with daidzin and puerarin causes differences in the β -CD structure and hence different host–guest binding modes. The last snapshots of the β -CD/D and β -CD/P complex in 20% n-PrOH after a 10-ns simulation are shown in Figure 8. A ternary complex between β -CD/guest and n-PrOH is formed involving water molecules. For β -CD/D the methyl of n-PrOH is inserted into the cavity and the hydroxyl of n-PrOH directly forms hydrogen bonds with daidzin and β -CD at the same time (Figure 8a). For β -CD/P the methyl of n-PrOH stays near the cavity boundary and the hydroxyl of n-PrOH hydrogen bonds to puerarin and β -CD with a local participation of water molecules (Figure 8b). Daidzin is embedded more deeply within the cavity with respect to the secondary rim than puerarin (Figure 8, panels c and d). On the contrary, daidzin and puerarin are both deeply inserted into the cavity in pure water, similar to Figure 8c. In 20% MeOH puerarin also gets out of the cavity in part but binds more tightly to β -CD (not shown here). In all 20% alcohol solutions studied daidzin stays within the cavity and shows a stronger ternary complex, such as β -CD/D/n-PrOH (Figure 8a).

3.5. Retention of Guest and Structural Explanation.

The retention times of daidzin (D) and puerarin (P) on the β -CD-coupled medium using alcohol–water mixtures as eluents are listed in Table 2. A longer retention time means stronger interaction of the analyte (D or P) with the medium.

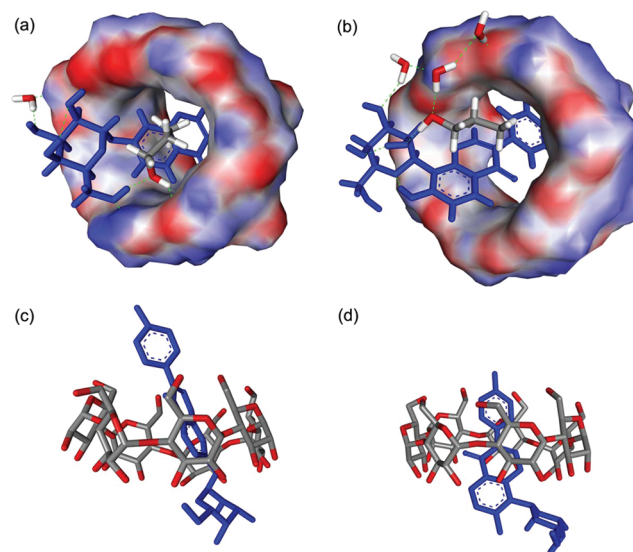


Figure 8. Last snapshot of β -CD/D (a) and β -CD/P (b) complexes in 20% n-PrOH. β -CD is represented by a solvent surface model with a probe radius of 0.14 nm colored by electrostatic potential. Guest molecules are marked in blue. Stick models of n-PrOH and water are colored by element. The dashed green lines indicate hydrogen bonds. The bottom snapshots (c and d) are the same as the top ones, with removal of solvent molecules and hydrogen atoms for clarity.

The retention time of the void mark (1% acetone) is 4.10 min, implying no retention of the analyte. In higher concentration D and P are eluted with a retention time close to 4 min, indicating a very weak interaction of D and P with the medium, and there are no significant differences between D and P. Interestingly, there is a slight increase in retention using pure alcohols (EtOH, i-PrOH, and n-PrOH) as eluents. The retention of P is slightly stronger than D in higher alcohol concentrations. A minimum for the retention time is observed in EtOH, i-PrOH, and n-PrOH eluents with higher concentration. As the alcohol concentration decreases, retentions of D and P both increase and are more sensitive to alcohol concentrations. Big differences between D and P occur in 50% MeOH, 29% EtOH, 20% i-PrOH, and 15% n-PrOH where the retention time of D is longer than P, revealing a stronger interaction of D with the medium than P.

A structural explanation for these experiments can be deduced from the MD results. In higher concentration the β -CD cavity is almost completely occupied by alcohol, and thus guest molecules (D or P) have low probability to be incorporated into the cavity. In this case, hydrogen bonding between β -CD and guests is the driving force responsible for the retention. MD simulations in pure alcohols show that alcohol does not interrupt hydrogen bonds between adjacent secondary hydroxyls. Similarly, we speculate that alcohol also does not interrupt hydrogen bonds between β -CD and guests in experiments. Puerarin with a hydroxyl group connected to the A ring, which is different from daidzin (Figure 1, panels c and d), favors more hydrogen bonds. Therefore, when using pure alcohols as eluents there is a slight increase in retention and puerarin shows a slightly stronger interaction with the medium.

In lower concentration the β -CD cavity is partly occupied by alcohol and guests have more of a chance to enter the cavity. Because the alcohol with lower polarity such as i-PrOH and n-PrOH can reside within the cavity for a longer time as discussed in section 3.2, guest molecules are not so easily inserted into the cavity in i-PrOH and n-PrOH as they are in MeOH and EtOH. Now the driving force between guest and

Table 2. Retention Time (min) of Daidzin (D) and Puerarin (P) on the β -CD-Coupled Medium Using Aqueous Alcohol Eluents with Varied Alcohol Concentration^a

eluent (v/v)	MeOH		EtOH		i-PrOH		n-PrOH	
	D	P	D	P	D	P	D	P
100%	4.26	4.17	4.48	4.66	5.96	6.28	4.94	5.11
90%	4.53	4.26	4.19	4.44	4.23	4.27	4.06	4.04
80%	4.99	4.56	4.20	4.60	4.08	4.15	3.90	3.99
70%	6.03	5.26	4.32	4.89	4.02	4.20	3.83	4.02
60%	8.79	6.93			4.10	4.31	3.85	4.30
50%	18.27	11.48			4.36	4.57	3.97	4.57
40%	>50	23.57	6.59	5.13	5.06	5.14	4.30	5.03
30%			12.88	7.71	7.73	7.35	5.16	6.11
29%			34.66	13.30				
28%					8.61	8.38		
26%					10.21	10.14		
24%					15.77	12.36		
20%					25.38	17.41	9.62	10.25
18%							13.72	10.45
15%							26.55	16.81

^aEach point was repeated three times, and the average values were given here. Relative standard deviations are less than 2%.

host changes to be the hydrophobic interaction although hydrogen-bonding interactions still exist. β -CD behaves as a rigid structure in i-PrOH and n-PrOH, which limits puerarin to be embedded deeply within the cavity and hence causes a weaker host–guest interaction. Daidzin has a more linear structure (Figure 1d) and thus can enter the cavity more easily even if it is rigid. In MeOH and EtOH the flexible β -CD may allow a tighter host–guest complex. With daidzin inside the cavity, β -CD is more flexible than with puerarin and β -CD has a stronger interaction with daidzin.

In this work we did not consider the medium effect on the structural deformation of β -CD. In the experiments β -CD was coupled to the polymer particle and the whole geometry is most likely somewhat different from free β -CD in solution. The medium may also limit the macrocycle flexibility and diminish to some extent effects of guests and solvents on the β -CD structure. If so, this rigidity might weaken interactions between the medium and the target analyte somewhat. Alcohol solutions have been studied at length using dielectric relaxation^{61–64} and molecular simulation.^{65–67} These binary mixtures are rather complex, and for instance, the hydrogen bond breaking energy has been estimated to be almost independent of the mixture composition whereas the corresponding enthalpy is much higher in water-depleted than in water-rich mixtures.⁶⁶ Hence there is a strong temperature dependence on the properties of such mixtures, which may also affect solutions containing CD and CD/guest complexes. Also, the viscosity of alcohol solutions (MeOH, EtOH and n-PrOH) at intermediate concentrations is significantly higher than for pure liquids.⁶⁵ The eluent with a higher viscosity might go against diffusion of the guest (puerarin or daidzin) to the stationary phase and lead to weaker interactions of guests with the media. Therefore, various factors contribute to the retention mechanism of puerarin and daidzin with the β -CD-coupled medium and they should be taken into consideration for a comprehensive understanding of such experiments.

4. CONCLUSIONS

Molecular dynamics (MD) simulations of free beta-cyclodextrin (β -CD) and the β -CD/puerarin and β -CD/daidzin complexes in alcohol solutions containing either methanol, ethanol, 2-propanol, or 1-propanol in different concentrations indicate

that there are structural deformations of β -CD, which depend on the alcohol concentration and on the type of alcohol and guest. Compared to water, higher concentrations of alcohol endow free β -CD with a more rigid structure, whereas lower concentrations of methanol and ethanol give a more flexible one. The rigidity may prevent puerarin from being deeply embedded within the β -CD cavity and hence causes a weaker ternary complex (β -CD/puerarin/alcohol). Alcohol residence within the cavity and solvent distribution highlight the most important properties of β -CD: a hydrophobic cavity and a hydrophilic surface. Finally we report the retention behavior of puerarin and daidzin on the β -CD-coupled stationary phase using alcohol–water mixtures as the mobile phases and give a structural explanation based on the MD results. We think this work provides valuable insights into ternary complexes involving β -CD/guest and alcohol molecules.

■ AUTHOR INFORMATION

Corresponding Author

*Tel.: +86-10-64416691. Fax: +86-10-64715443. E-mail: twtan@mail.buct.edu.cn.

Notes

The authors declare no competing financial interest.

■ ACKNOWLEDGMENTS

The authors thank Professor Torgny Fornstedt for inviting H.Z. to perform this study in Uppsala University, Professor Jan-Christer Janson and Jerry Stahlberg for technical assistance, and Cong Li and Rong Li for helpful discussion. Chinese Scholarship Council (CSC) is acknowledged for providing scholarship for H.Z. This research was supported by the National Natural Science Foundation of China (21076017, 20876011), 863 program (2007AA100404), 973 program (2009CB24703, 2011CB710805), Beijing Municipal Science & Technology Commission (Z09010300840901), and special funds of cooperation project of Beijing Municipal Education Commission.

■ REFERENCES

- (1) Del Valle, E. M. M. *Process Biochem.* 2004, 39, 1033–1046.

- (2) Szejtli, J. *Chem. Rev.* **1998**, *98*, 1743–1753.
- (3) Connors, K. A. *Chem. Rev.* **1997**, *97*, 1325–1357.
- (4) Julian, C.; Miranda, S.; Zapata-Torres, G.; Mendizabal, F.; Olea-Azar, C. *Biorg. Med. Chem.* **2007**, *15*, 3217–3224.
- (5) Dodziuk, H. *J. Mol. Struct.* **2002**, *614*, 33–45.
- (6) Ritter, H.; Jazkewitsch, O.; Mondryk, A.; Staffel, R. *Macromolecules* **2011**, *44*, 1365–1371.
- (7) Marcy, J. E.; Koontz, J. L.; O'Keefe, S. F.; Duncan, S. E. *J. Agric. Food. Chem.* **2009**, *57*, 1162–1171.
- (8) Buschmann, H. J.; Schollmeyer, E. *J. Cosmet. Sci.* **2002**, *53*, 185–191.
- (9) Liu, W. P.; Zhou, S. S.; Wang, L. M.; Zhang, A. P.; Lin, K. D. *J. Agric. Food. Chem.* **2008**, *56*, 2708–2713.
- (10) Schneiderman, E.; Stalcup, A. M. *J. Chromatogr. B* **2000**, *745*, 83–102.
- (11) Wu, S. Z.; Xu, M. Y.; Zeng, F.; Yu, C. M. *Langmuir* **2010**, *26*, 4529–4534.
- (12) Li, X. Q.; Liang, K.; Wang, C. Y.; Bai, X. L.; Xu, J. Y.; Shen, J. C.; Liu, J. Q. *J. Mol. Catal. A: Chem.* **2008**, *295*, 47–51.
- (13) Saenger, W.; Noltemeyer, M.; Manor, P. C.; Hingerty, B.; Klar, B. *Biorg. Chem.* **1976**, *5*, 187–195.
- (14) Shin, K.-m.; Dong, T.; He, Y.; Taguchi, Y.; Oishi, A.; Nishida, H.; Inoue, Y. *Macromol. Biosci.* **2004**, *4*, 1075–1083.
- (15) Ellis, A. V.; Chong, S.; Jansen, M. *J. Incl. Phenom. Macrocycl. Chem.* **2009**, *63*, 267–272.
- (16) Raffaini, G.; Ganazzoli, F.; Malpezzi, L.; Fuganti, C.; Fronza, G.; Panzeri, W.; Mele, A. *J. Phys. Chem. B* **2009**, *113*, 9110–9122.
- (17) Zukowski, J.; Sybilkska, D.; Jurczak, J. *Anal. Chem.* **1985**, *57*, 2215–2219.
- (18) Zeng, Z. R.; Tian, Y.; Zhong, C.; Fu, E. Q. *J. Chromatogr. A* **2009**, *1216*, 1000–1007.
- (19) Gazdag, M.; Szepesi, G.; Huszar, L. *J. Chromatogr.* **1986**, *371*, 227–234.
- (20) Liu, Y.; Song, Y.; Chen, Y.; Yang, Z. X.; Ding, F. *J. Phys. Chem. B* **2005**, *109*, 10717–10726.
- (21) Nelson, G.; Patonay, G.; Warner, I. M. *Anal. Chem.* **1988**, *60*, 274–279.
- (22) Hamai, S. *J. Phys. Chem.* **1989**, *93*, 2074–2078.
- (23) Liao, Y.; Bohne, C. *J. Phys. Chem.* **1996**, *100*, 734–743.
- (24) Zifferer, G.; Sellner, B.; Kornherr, A.; Krois, D.; Brinker, U. H. *J. Phys. Chem. B* **2008**, *112*, 710–714.
- (25) Lipkowitz, K. B. *Chem. Rev.* **1998**, *98*, 1829–1873.
- (26) Raffaini, G.; Ganazzoli, F. *Chem. Phys.* **2007**, *333*, 128–134.
- (27) Winkler, R. G.; Fioravanti, S.; Ciccotti, G.; Margheritis, C.; Villa, M. *J. Comput. Aided Mol. Des.* **2000**, *14*, 659–667.
- (28) Jana, M.; Bandyopadhyay, S. *J. Phys. Chem. B* **2011**, *115*, 6347–6357.
- (29) Jana, M.; Bandyopadhyay, S. *Langmuir* **2009**, *25*, 13084–13091.
- (30) Cai, W.; Sun, T.; Shao, X.; Chipot, C. *Phys. Chem. Chem. Phys.* **2008**, *10*, 3236–43.
- (31) Naidoo, K. J.; Chen, J. Y. J.; Jansson, J. L. M.; Widmalm, G.; Maliniak, A. *J. Phys. Chem. B* **2004**, *108*, 4236–4238.
- (32) Naidoo, K. J.; Gamielidien, M. R.; Chen, J. Y. J.; Widmalm, G.; Maliniak, A. *J. Phys. Chem. B* **2008**, *112*, 15151–15157.
- (33) Boonyaratpanakalin, K. S.; Wolschann, P.; Lawtrakul, L. *J. Incl. Phenom. Macrocycl. Chem.* **2011**, *70*, 279–290.
- (34) Keung, W. M.; Vallee, B. L. *Phytochemistry* **1998**, *47*, 499–506.
- (35) Li, R.; Zhao, R.; Zhang, H.; Li, C.; Feng, D.; Qin, P.; Tan, T. *Chromatographia* **2010**, *72*, 47–54.
- (36) Sharff, A. J.; Rodseth, L. E.; Quiocho, F. A. *Biochemistry* **1993**, *32*, 10553–10559.
- (37) Frisch, M. J.; Trucks, G. W.; Schlegel, H. B.; Scuseria, G. E.; Robb, M. A.; Cheeseman, J. R.; Montgomery, J. A., Jr.; Vreven, T.; Kudin, K. N.; Burant, J. C.; Millam, J. M.; Iyengar, S. S.; Tomasi, J.; Barone, V.; Mennucci, B.; Cossi, M.; Scalmani, G.; Rega, N.; Petersson, G. A.; Nakatsuji, H.; Hada, M.; Ehara, M.; Toyota, K.; Fukuda, R.; Hasegawa, J.; Ishida, M.; Nakajima, T.; Honda, Y.; Kitao, O.; Nakai, H.; Klene, M.; Li, X.; Knox, J. E.; Hratchian, H. P.; Cross, J. B.; Bakken, V.; Adamo, C.; Jaramillo, J.; Gomperts, R.; Stratmann, R. E.; Yazayev, O.; Austin, A. J.; Cammi, R.; Pomelli, C.; Ochterski, J. W.; Ayala, P. Y.; Morokuma, K.; Voth, G. A.; Salvador, P.; Dannenberg, J. J.; Zakrzewski, V. G.; Dapprich, S.; Daniels, A. D.; Strain, M. C.; Farkas, O.; Malick, D. K.; Rabuck, A. D.; Raghavachari, K.; Foresman, J. B.; Ortiz, J. V.; Cui, Q.; Baboul, A. G.; Clifford, S.; Cioslowski, J.; Stefanov, B. B.; Liu, G.; Liashenko, A.; Piskorz, P.; Komaromi, I.; Martin, R. L.; Fox, D. J.; Keith, T.; Al-Laham, M. A.; Peng, C. Y.; Nanayakkara, A.; Challacombe, M.; Gill, P. M. W.; Johnson, B.; Chen, W.; Wong, M. W.; Gonzalez, C.; Pople, J. A. Gaussian 03, revision C.02; Gaussian, Inc.: Wallingford, CT, 2004.
- (38) Case, D. A.; Darden, T. A.; Cheatham, T. E.; I. I. I.; Simmerling, C. L.; Wang, J.; Duke, R. E.; Luo, R.; Crowley, M.; Walker, R. C.; Zhang, W.; Merz, K. M.; Wang, B.; Hayik, S.; Roitberg, A.; Seabra, G.; Kolossváry, I.; Wong, K. F.; Paesani, F.; Vanicek, J.; Wu, X.; Brozell, S. R.; Steinbrecher, T.; Gohlke, H.; Yang, L.; Tan, C.; Mongan, J.; Hornak, V.; Cui, G.; Mathews, D. H.; Seetin, M. G.; Sagui, C.; Babin, V.; and Kollman, P. A. AMBER 10; University of California: San Francisco, CA, 2008.
- (39) Kirschner, K. N.; Yongye, A. B.; Tschampel, S. M.; González-Outeiriño, J.; Daniels, C. R.; Foley, B. L.; Woods, R. J. *J. Comput. Chem.* **2008**, *29*, 622–655.
- (40) Wang, J. M.; Wolf, R. M.; Caldwell, J. W.; Kollman, P. A.; Case, D. A. *J. Comput. Chem.* **2004**, *25*, 1157–1174.
- (41) Mobley, D. L.; Chodera, J. D.; Dill, K. A. *J. Chem. Phys.* **2006**, *125*, 084902.
- (42) Sorin, E. J.; Pande, V. S. *Biophys. J.* **2005**, *88*, 2472–2493.
- (43) DePaul, A. J.; Thompson, E. J.; Patel, S. S.; Haldeman, K.; Sorin, E. J. *Nucleic Acids Res.* **2010**, *38*, 4856–4867.
- (44) Duan, Y.; Wu, C.; Chowdhury, S.; Lee, M. C.; Xiong, G. M.; Zhang, W.; Yang, R.; Cieplak, P.; Luo, R.; Lee, T.; Caldwell, J.; Wang, J. M.; Kollman, P. *J. Comput. Chem.* **2003**, *24*, 1999–2012.
- (45) Kirschner, K. N. *Proc. Natl. Acad. Sci.* **2001**, *98*, 10541–10545.
- (46) Lindner, K.; Saenger, W. *Carbohydr. Res.* **1982**, *99*, 103–115.
- (47) Jorgensen, W. L.; Chandrasekhar, J.; Madura, J. D.; Impey, R. W.; Klein, M. L. *J. Chem. Phys.* **1983**, *79*, 926–935.
- (48) van der Spoel, D.; Lindahl, E.; Hess, B.; Groenhof, G.; Mark, A. E.; Berendsen, H. J. C. *J. Comput. Chem.* **2005**, *26*, 1701–1718.
- (49) Hess, B.; Kutzner, C.; van der Spoel, D.; Lindahl, E. *J. Chem. Theory Comput.* **2008**, *4*, 435–447.
- (50) Bussi, G.; Donadio, D.; Parrinello, M. *J. Chem. Phys.* **2007**, *126*.
- (51) Parrinello, M.; Rahman, A. *J. Appl. Phys.* **1981**, *52*, 7182–7190.
- (52) Nose, S.; Klein, M. L. *Mol. Phys.* **1983**, *50*, 1055–1076.
- (53) Essmann, U.; Perera, L.; Berkowitz, M. L.; Darden, T.; Lee, H.; Pedersen, L. G. *J. Chem. Phys.* **1995**, *103*, 8577–8593.
- (54) Darden, T.; York, D.; Pedersen, L. *J. Chem. Phys.* **1993**, *98*, 10089–10092.
- (55) Hess, B.; Bekker, H.; Berendsen, H. J. C.; Fraaije, J. G. E. M. *J. Comput. Chem.* **1997**, *18*, 1463–1472.
- (56) Miyamoto, S.; Kollman, P. A. *J. Comput. Chem.* **1992**, *13*, 952–962.
- (57) Tetko, I. V.; Tanchuk, V. Y. *J. Chem. Inf. Comput. Sci.* **2002**, *42*, 1136–1145.
- (58) Tetko, I. V.; Tanchuk, V. Y.; Villa, A. E. P. *J. Chem. Inf. Comput. Sci.* **2001**, *41*, 1407–1421.
- (59) Zhang, H. Y.; Feng, W.; Li, C.; Tan, T. W. *J. Phys. Chem. B* **2010**, *114*, 4876–4883.
- (60) Betzel, C.; Saenger, W.; Hingerty, B. E.; Brown, G. M. *J. Am. Chem. Soc.* **1984**, *106*, 7545–7557.
- (61) Sato, T.; Chiba, A.; Nozaki, R. *J. Chem. Phys.* **2000**, *112*, 2924–2932.
- (62) Sato, T.; Chiba, A.; Nozaki, R. *J. Chem. Phys.* **1999**, *110*, 2508–2521.
- (63) Sato, T.; Chiba, A.; Nozaki, R. *J. Chem. Phys.* **2000**, *113*, 9748–9758.
- (64) Sato, T.; Buchner, R. *J. Chem. Phys.* **2003**, *118*, 4606–4613.

- (65) Wensink, E. J. W.; Hoffmann, A. C.; van Maaren, P. J.; van der Spoel, D. *J. Chem. Phys.* **2003**, *119*, 7308–7317.
- (66) van der Spoel, D.; van Maaren, P. J.; Larsson, P.; Timneanu, N. *J. Phys. Chem. B* **2006**, *110*, 4393–4398.
- (67) van der Spoel, D.; Wensink, E. J. W.; Hoffmann, A. C. *Langmuir* **2006**, *22*, 5666–5672.